

1, 6-O, O-Diacetylbritannilactone from *Inula britannica* Induces Anti-Tumor Effect on Oral Squamous Cell Carcinoma via miR-1247-3p/LXR α /ABCA1 Signaling

This article was published in the following Dove Press journal:
OncoTargets and Therapy

Shaohua Zheng^{1,*}
Lihua Li^{2,*}
Na Li³
Yi Du⁴
Nan Zhang⁵

¹Department of Anesthesiology, The First Affiliated Hospital of Xi'an Jiaotong University, Xi'an City, Shanxi Province, 710061, People's Republic of China;

²Department of Stomatology, North Sichuan Medical College, Nanchong, Sichuan Province, 637000, People's Republic of China; ³Department of Stomatology, Xi'an Shiyou University Hospital, Xi'an City, Shanxi Province, 710065, People's Republic of China;

⁴Jinan Stomatological Hospital, Jinan City, Shandong Province 250001, People's Republic of China; ⁵Department of Stomatology, The First Affiliated Hospital of Xi'an Jiaotong University, Xian City, Shanxi Province 710061, People's Republic of China

*These authors contributed equally to this work

Correspondence: Yi Du
Jinan Stomatological Hospital, Jinan City, Shandong Province 250001, People's Republic of China
Email yidu1967@163.com

Nan Zhang
Department of Stomatology, The First Affiliated Hospital of Xi'an Jiaotong University, Xi'an City, Shanxi Province 710061, People's Republic of China
Email rq6773@163.com

Introduction: Oral squamous cell carcinoma (OSCC) is the most prevalent malignancy affecting the oral cavity and is associated with severe morbidity and high mortality. 1, 6-O, O-Diacetylbritannilactone (OODBL) isolated from the medicinal herb of *Inula britannica* has various biological activities such as anti-inflammation and anti-cancer. However, the effect of OODBL on OSCC progression remains unclear. Here, we were interested in the function of OODBL in the development of OSCC.

Methods: The effect of OODBL on OSCC progression was analyzed by MTT assays, colony formation assays, transwell assays, apoptosis analysis, cell cycle analysis, and in vivo tumorigenicity analysis. The mechanism investigation was performed by qPCR assays, Western blot analysis, and luciferase reporter gene assays.

Results: We found that OODBL inhibits the proliferation of OSCC cells in vitro. Moreover, the migration and invasion were attenuated by OODBL treatment in the OSCC cells. OODBL arrested cells at the G0/G1 phase and induced cell apoptosis. OODBL was able to up-regulate the expression of LXR α , ABCA1, and ABCG1 in the system. In addition, OODBL activated LXR α /ABCA1 signaling by targeting miR-1247-3p. Furthermore, the expression levels of cytochrome c in the cytoplasm, cleaved caspase-9, and cleaved caspase-3 were dose-dependently reduced by OODBL. Besides, OODBL increased the expression ratio of Bax to Bcl-2. Moreover, OODBL repressed tumor growth of OSCC cells in vivo.

Discussion: Thus, we conclude that OODBL inhibits OSCC progression by modulating miR-1247-3p/LXR α /ABCA1 signaling. Our finding provides new insights into the mechanism by which OODBL exerts potent anti-tumor activity against OSCC. OODBL may be a potential anti-tumor candidate, providing a novel clinical treatment strategy of OSCC.

Keywords: OSCC, OODBL, anti-tumor, LXR α /ABCA1 signaling, miR-1247-3p

Introduction

Head and neck cancer (HNC) contains a collection of malignancies that influence the pharynx, larynx, and oral cavity,¹ with about 600,000 newly diagnosed patients and around 300,000 mortalities annually.² Oral squamous cell carcinoma (OSCC) is the most prevalent lethal tumor of HNCs and the sixth most common cancer globally and estimates approximately 90% of all the oral carcinomas.^{3,4} OSCC is a destructive illness that first manifests as a painless lump in the mouth that might

influence oral functions, including speech and swallowing, if displayed at superior stages.^{5,6} The occurrence frequencies of OSCC in both males and females in all public cancer registries are huge worldwide.⁷ OSCC can stem from various subsites, including the floor of the mouth, alveolar ridge, lips, buccal mucosa, retromolar trigone, hard palate, and oral tongue.^{8,9} The traditional treatment of advanced-grade OSCC can always have harmful impacts on patients' physiologic capacities and appearance, and even leads to fatality.^{10,11} Hence, the new anti-OSCC candidates are urgently needed. However, the investigation in this field is poorly advanced.

Medicinal plants are applied for the treatment of various diseases in Japan, Korea, China, and other Asian regions such as Vietnam and Malaysia, and now all over the world.¹² *Inula britannica* is a useful therapeutic herb traditionally employed in back pain and arthritis in populace medication.^{13,14} *Inula britannica* is a sort of plant in the species *Inula* in the Asteraceae genus with the meadow fleabane or British yellowhead.¹⁵ Herbs belonging to the *Inula* are recognized for their distinct biological activities, including anti-inflammatory, cytotoxic, hepatoprotective, antimicrobial, and anti-cancer properties.^{16,17} Many chemical compounds have been extracted from *Inula britannica*, including flavonoids, phenolics, steroids, and 1, 6-O, O-Diacetylbritannilactone (OODBL).¹⁸ OODBL is a recognized sesquiterpene lactone (STL) with a motif of α -methylene- γ -lactone separated from the *Inula britannica* flower heads.¹⁹ It has been reported that OODBL represses mast cell activation and displays several biological effects such as anti-cancer and anti-inflammatory activities.^{20,21} OODBL induces an anti-tumor effect on leukemia cells by modulating MAPK pathway.²² However, the effect of OODBL on OSCC progression is still unreported.

Liver X receptor α (LXR α) serves as a nuclear hormone receptor, contributing to transcriptional activity by binding with lipophilic hormones such as thyroid and steroid hormones.²³ ATP-binding cassette transporter G1 and A1 (ABCG1 and ABCA1) is the lipid regulator that pumps phospholipid and cholesterol out of cells.²⁴ Inducement of ABCA1 and ABCG1 can cause cholesterol efflux acknowledged as lipid floats.²⁵ Furthermore, the transcription of ABCA1 and ABCG1 is regulated by LXR α .²⁶ The LXR α /ABCA1 signaling pathway plays a crucial role in multiple pathological processes, such as anti-inflammatory and anti-tumor reactions.²⁷⁻²⁹ It has been reported that LXR α /ABCA1 signaling reduces the cell proliferation of OSCC.³⁰ But whether LXR α /ABCA1

signaling is involved in the anti-tumor effect of OODBL remains unclear.

MicroRNAs (miRNAs) are identified as the small RNAs that typically modulate mRNAs' stability and translation, regulating genes referred to physiological and pathological processes such as cell cycle regulation, stress response, differentiation, inflammation, and cancer development.^{31,32} MiR-375 is involved in the invasion and proliferation regulation of OSCC.³³ It has been reported that miR-1247-3p provokes cancer-related activation of fibroblast to promote liver cancer lung metastasis.³⁴ Meanwhile, cytochrome c, cleaved caspase-9, cleaved caspase-3, Bcl-2, and Bax are involved in the modulation of apoptosis and can be served as apoptosis markers.³⁵⁻⁴⁰ However, whether OODBL targets these critical factors in cancer development remain elusive.

In this study, we aimed to explore the anti-tumor effect of OODBL on OSCC. We uncovered that OODBL inhibited the development of OSCC by modulating miR-1247-3p/LXR α /ABCA1 signaling in vitro and in vivo. Our finding provides new insights into the mechanism by which OODBL represses OSCC progression, providing valuable evidence of the OODBL function and novel therapeutic strategy of OSCC.

Materials and Methods

Cell Culture and Treatment

Normal oral cells (HOK cells) and Human oral squamous cell carcinoma cells, including CAL27 and SCC15 cell lines, were obtained in American Type Tissue Culture Collection. The cells were cultured in the medium of RPMI-1640 (Solarbio, China) containing 10% fetal bovine serum (Gibco, USA), 0.1 mg/mL streptomycin, and 100 units/mL penicillin at a condition of 37°C with 5% CO₂. The cells were treated with OODBL of indicated dose for 48 hours before further analysis. The OODBL (purity >98%) was obtained in Chuntest Biotechnology Co. Ltd (Shanghai, China).

MTT Assays

MTT assays measured the effects of the OODBL on cell proliferation of OSCC. Briefly, about 2×10^4 CAL27 and SCC15 cells were put into 96 wells and cultured for 12 hours. The cells were then added with various doses of OODBL for 24 h, 36 h, and 48 h. After treatment, the cells were added with a 10 μ L MTT solution (5 mg/mL) and cultured for an extra 4 h. Discarded medium and 150 μ L

DMSO was used to treat the wells. An ELISA browser was applied to analyze the absorbance at 570nm (Bio-Tek EL 800, USA).

Colony Formation Assays

About 1×10^3 CAL27 and SCC15 cells were layered in 6 wells and incubated in RPMI-1640 at 37°C. After two weeks, cells were cleaned with PBS Buffer, made in methanol about thirty minutes, and dyed with crystal violet dye at the dose of 1%, after which the number of colonies was calculated.

Transwell Assays

Transwell assays analyzed the impacts of the OODBL on cell invasion and migration of OSCC using a Transwell plate (Corning, NY) according to the manufacturer's instruction. Briefly, the upper chambers were plated with around 1×10^5 cells. Then, solidified through 4% paraformaldehyde and dyed with crystal violet. The invaded cells were recorded and calculated.

Analysis of Cell Apoptosis

Around 1×10^5 CAL27 and SCC15 cells were cultured on 6-well dishes and were employed with different concentrations of OODBL. Apoptosis-mediated cell death of tumor cells was measured by using an Annexin V-FITC/PI apoptosis detection kit (Keygen Biot Solasodine, China). Briefly, about 1×10^6 cells were washed and collected by binding buffer and were dyed with Annexin V-FITC and PI at 25°C, followed by the Flow cytometry analysis.

Cell Cycle Analysis

About 1×10^5 CAL27 and SCC15 cells were layered in 6-well dishes and employed with various doses of OODBL. The cells were gathered and solidified in paraformaldehyde at 4°C. The RNaseA (100 µg/mL) was used to treat the cells for about thirty minutes at 37°C, followed by the staining with PI (50 µg/mL) for about thirty minutes. And then, the flow cytometry was carried out, and the population of the cell cycle was examined by using the software of Multi-cycle.

Quantitative Reverse Transcription-PCR (qRT-PCR)

The total RNAs were extracted by TRIzol (Invitrogen, USA). The first-strand cDNA was synthesized as the

manufacturer's instruction (Invitrogen, USA). The qRT-PCR was conducted by employing the SYBR Premix Ex Taq II kit (Takara, Japan). The standard control for miRNA and mRNA was U6 and GAPDH, respectively. Quantitative determination of the RNA levels was performed in triplicate in three independent experiments. The primer sequences are as follows:

miR-1247-3p: forward: 5'-CTGGTGGTTTAGAGGATGT-3',

miR-1247-3p: reverse: 5'-GTCCTTGAACATCCGGGCG-3'

LXRα: forward: 5'-CCACCGAATGCGCGAACCT-3',

LXRα: reverse: 5'-GAGTCCATTACAGCGGTGCC-3'.

U6: forward: 5'-GACAGATTCGGTCTGTGGCAC-3'

U6: reverse: 5'-GATTACCCGTCGGCCATCGATC-3'

Western Blot Analysis

Total proteins were extracted from the cells or mice tissues with RIPA buffer (Beyotime, China). Protein concentrations were measured using the BCA Protein Quantification Kit (YEASEN, China). Identical quantities of protein were divided by SDS-PAGE, followed by the transfer to PVDF membranes (Millipore, USA). The membranes were hindered with 5% milk and hatched with first antibodies for LXRα (Abcam, Cambridge, MA) (1:1000), ABCA1 (Abcam, Cambridge, MA) (1:1000), ABCG1 (Abcam, Cambridge, MA) (1:1000), and β-actin (Abcam, Cambridge, MA)(1:1000) at 4°C overnight. Afterward, we exposed the membranes to related second antibodies for 1 hour, followed by the visualization using an imaging system of Bio-Rad. The results of Western blot analysis were quantified by ImageJ software.

Luciferase Reporter Gene Assay

The luciferase reporter gene assays were performed by using the Dual-luciferase Reporter Assay System (Promega, USA) was used to carry out the luciferase reporter gene assays. Briefly, the samples were treated with the inhibitor of miR-1247-3p, mimics, or miR-control, the vector containing LXRα fragment, using Lipofectamine 2000 (Invitrogen, USA), followed by the analysis of luciferase activities, in which Renilla was applied as a normalized control.

Analysis of Tumorigenicity in Nude Mice

The effect of OODBL on neoplasm extension in vivo was analyzed in nude mice of Balb/c. To establish an in vivo

tumor model, about 1×10^7 cells were subcutaneously injected in the mice. We randomly separated the mice into two groups ($n=3$), including mock and OODBL treatment groups. The mice were intragastrically furnished with OODBL (0.1 mL/10g) or normal saline in the corresponding group daily. After ten days of injection, we measured tumor growth every five days. We sacrificed the mice after thirty days of injection, and tumors were scaled. Tumor volume (V) was observed by estimating the length and width with calipers and measured with the method $\times 0.5$. The expression levels of Ki-67 of the tumor tissues were tested by immunohistochemical staining with the Ki-67 antibody (Santa Cruz Biotechnology, USA). The protein expression levels of LXR α , ABCA1, and ABCG1 were analyzed by Western blot analysis in tumor tissues. Animal care and method procedure were authorized by the Animal Ethics Committee of Jinan Stomatological Hospital. All animal procedures were performed in accordance with the Guidelines for Care and Use of Laboratory Animals of "The First Affiliated Hospital of Xi'an Jiaotong University" and approved by the Animal Ethics Committee of "Animal Ethical and Welfare Committee (AEWC)".

Statistical Analysis

Data were expressed as means \pm SEM, and all experiments were replicated at least three times. Statistical analysis was conducted using SPSS software. The significance was examined by one-way analysis followed by *t*-test. $P < 0.05$ were judged statistically significant.

Results

OODBL Inhibits the Proliferation of OSCC Cells

To assess the effect of OODBL on the progression of OSCC, we synthesized OODBL, and the structural formula is shown in Figure 1. Then, we analyzed the function of OODBL in modulating the proliferation of OSCC cells, including CAL27 and SCC15 cells. MTT assays revealed that OODBL significantly suppressed the cell viability in a dose-dependent and time-dependent manner in the CAL27 ($P < 0.01$) (Figure 2A) and SCC15 cells ($P < 0.01$) (Figure 2B), suggesting that OODBL induces an inhibitory influence on the proliferation of OSCC cells. Similarly, OODBL dose-dependently reduced the colony formation of OSCC cells, such as CAL27 ($P < 0.01$) (Figure 2C) and SCC15 cells ($P < 0.01$) (Figure 2D),

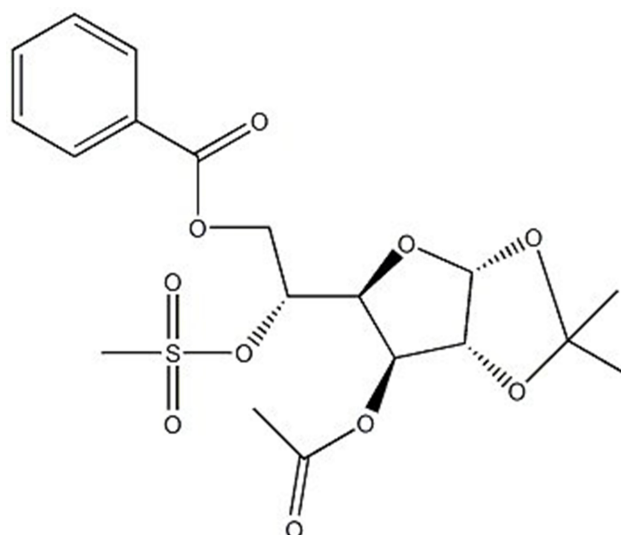


Figure 1 The structural formula of OODBL.

confirming that OODBL inhibits the OSCC cell proliferation *in vitro*.

OODBL Impairs the OSCC Cell Migration and Invasion

Next, we further explored the role of OODBL in the invasion and migration of OSCC cells. The OSCC cells were treated with OODBL at the indicated dose for 48 hours. Transwell assays demonstrated that the OODBL treatment remarkably repressed the migration of CAL27 and SCC15 cells in a dose-dependent manner ($P < 0.01$) (Figure 3A). We also observed that the invasion of CAL27 and SCC15 cells was dose-dependently reduced by OODBL ($P < 0.01$) (Figure 3B), indicating that OODBL restrains the migration and invasion of OSCC cells.

OODBL Modulates Cell Cycle and Apoptosis in OSCC Cells

We were then concerned about the effect of OODBL on cell cycle and apoptosis in OSCC cells, such as CAL27 and SCC15 cells. Significantly, with the increase of OODBL concentration, the cell distribution of the G0/G1 phase was enhanced, whereas cell distribution in S phase cells and G2/M phase was decreased, implying that OODBL arrests OSCC cells at G0/G1 phase ($P < 0.01$) (Figure 4A). Furthermore, the quantitative analysis of flow cytometry with PI staining showed that OODBL promoted the apoptosis of CAL27 and SCC15 cells in a dose-dependent way ($P < 0.01$) (Figure 4B), suggesting that OODBL affects cell apoptosis of OSCC.

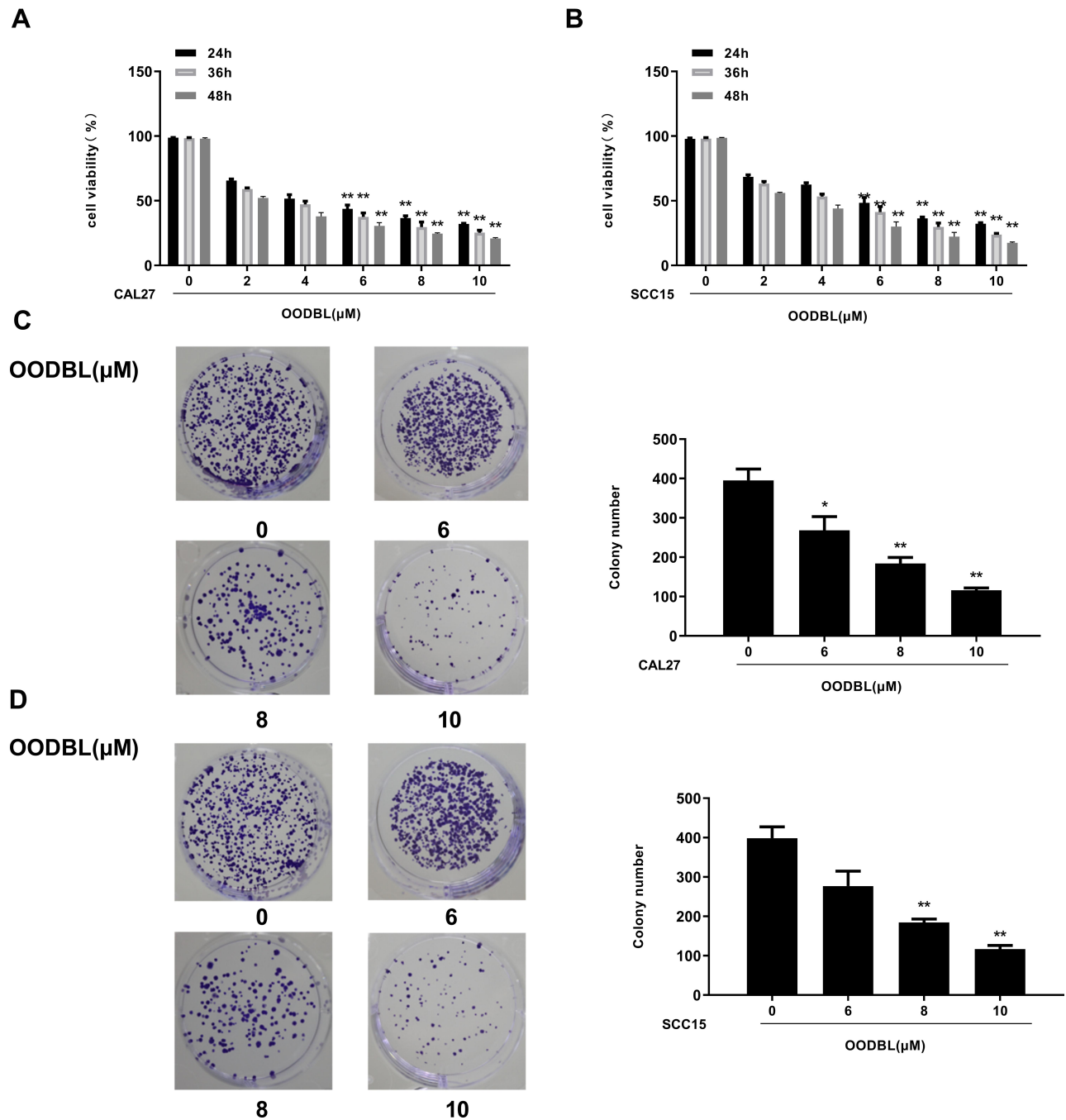


Figure 2 OODBL inhibits the proliferation of OSCC cells. (A and B) The effect of OODBL on cell viability was measured by MTT assays in the CAL27 and SCC15 cells treated with OODBL of indicated dose, respectively. (C and D) The effect of OODBL on cell proliferation was analyzed by colony formation assays in the CAL27 and SCC15 cells treated with OODBL of indicated dose, respectively.

Notes: n=3, means ± SD, compared with the control group, * $p < 0.05$, ** $p < 0.01$.

OODBL Activates LXR α /ABCA1 Signaling by Targeting miR-1247-3p

Next, we further investigated the underlying mechanism of OODBL inhibiting OSCC development. Western blot analysis (Figure 5A) with the quantification (Figure 5B)

exhibited that OODBL significantly activated the expression of LXR α , ABCA1, and ABCG1 in the CAL27 cells ($P < 0.01$), implying that OODBL may exert its anti-OSCC role by modulating LXR α /ABCA1 signaling.

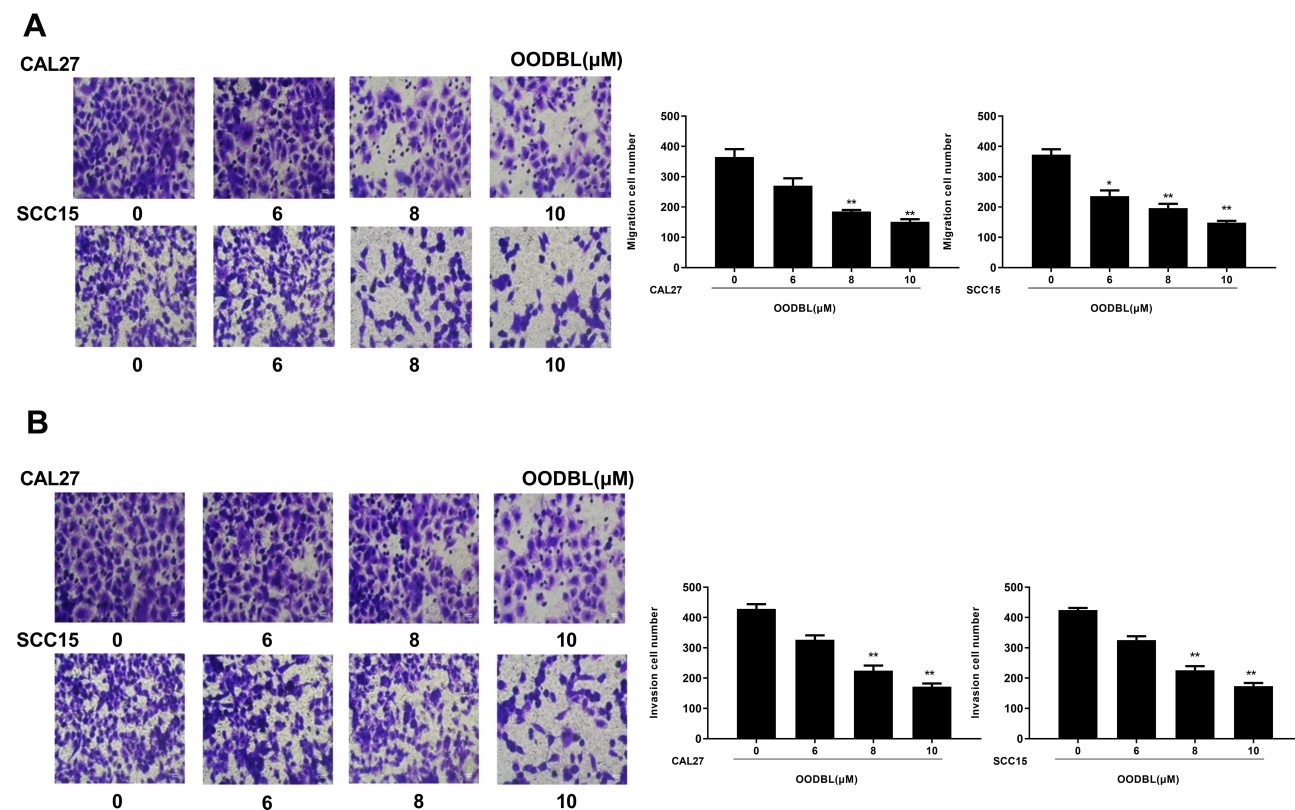


Figure 3 OODBL impairs the migration and invasion of OSCC cells. **(A)** The effect of OODBL on cell migration was tested by Transwell assays in the CAL27 and SCC15 cells treated with OODBL of indicated dose. **(B)** The effect of OODBL on cell invasion was assessed by Transwell assays in the CAL27 and SCC15 cells treated with OODBL of indicated dose.

Notes: n=3, means \pm SD, compared with the control group. * $p < 0.05$, ** $p < 0.01$.

Then, we tried to explore the specific mechanism of OODBL mediating LXR α /ABCA1 signaling. Fundamentally, we identified that miR-1247-3p was able to potentially target to LXR α in a bioinformatic analysis by Targetscan (http://www.targetscan.org/vert_72/) (Figure 6A). Luciferase reporter gene assays revealed that miR-1247-3p mimic attenuated the luciferase activity of wild type LXR α ($P < 0.01$) but failed to affect LXR α with miR-1247-3p binding site mutant in the CAL27 cells (Figure 6B), verifying that miR-1247-3p may specifically target to LXR α . Meanwhile, the intuitive expression of miR-1247-3p was analyzed in the OSCC cells ($P < 0.01$) (Figure 6C). The expression levels of LXR α were remarkably decreased by miR-1247-3p mimic ($P < 0.01$), while the mRNA (Figure 6D) and protein (Figure 6E) expression levels of LXR α were significantly increased by the inhibitor of miR-1247-3p in the CAL27 cells ($P < 0.01$), suggesting that miR-1247-3p is able to inhibit the expression of LXR α . Furthermore, OODBL could down-regulate the expression levels of the miR-1247-3p in a dose-

dependent manner in the cells ($P < 0.01$) (Figure 6F). Together these data indicate that OODBL activates LXR α /ABCA1 signaling by targeting miR-1247-3p.

OODBL Affects Cytochrome C and Caspases Activities in OSCC Cells

Next, we were interested in how the OODBL affected the apoptosis of OSCC cells. The expression levels of cytochrome c in the cytoplasm, cleaved caspase-9 (c-caspase-9) and cleaved caspase-3 (c-caspase-3) were dose-dependently reduced by OODBL in CAL27 cells ($P < 0.01$) (Figure 7A), implying that the inhibition of cytochrome c release from the mitochondria to cytoplasm and the expression of c-caspase-9 and c-caspase-3 were involved in the apoptosis of OSCC cells mediated by OODBL. Besides, OODBL reduced the expression of Bcl-2, but increased the expression of Bax in the CAL27 cells ($P < 0.01$) (Figure 7B), indicating that the Bcl-2 and Bax are involved in OODBL-induced OSCC cell apoptosis.

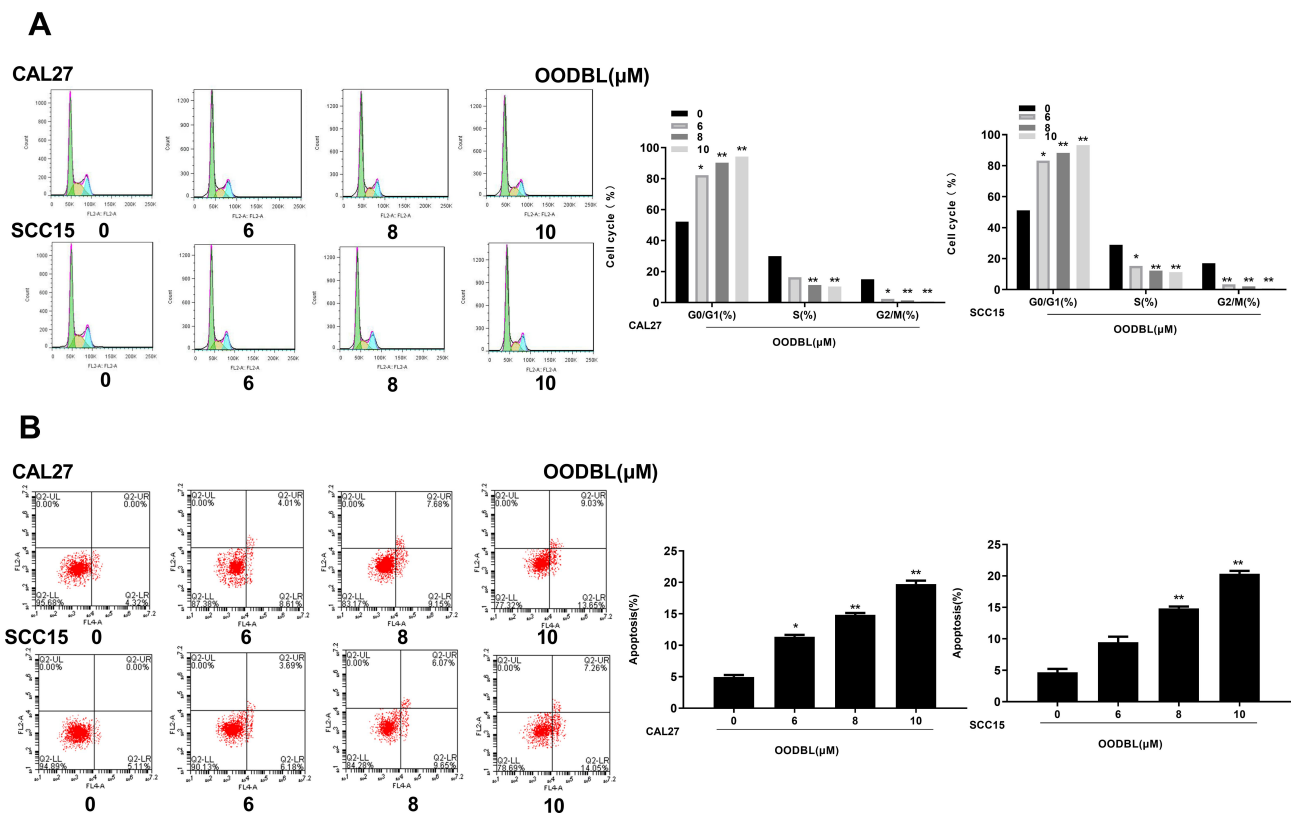


Figure 4 OODBL modulates cell cycle and apoptosis in OSCC cells. **(A)** The effect of OODBL on cell cycle was measured by flow cytometry in the CAL27 and SCC15 cells treated with OODBL of indicated dose. The percentages of cells in the G1, S, and G2/M phases were calculated using the Multi-cycle software, respectively. **(B)** The effect of OODBL on cell apoptosis was analyzed by flow cytometry in the CAL27 and SCC15 cells treated with OODBL of indicated dose. **Notes:** n=3, means ± SD, compared with the control group, **p* < 0.05, ***p* < 0.01.

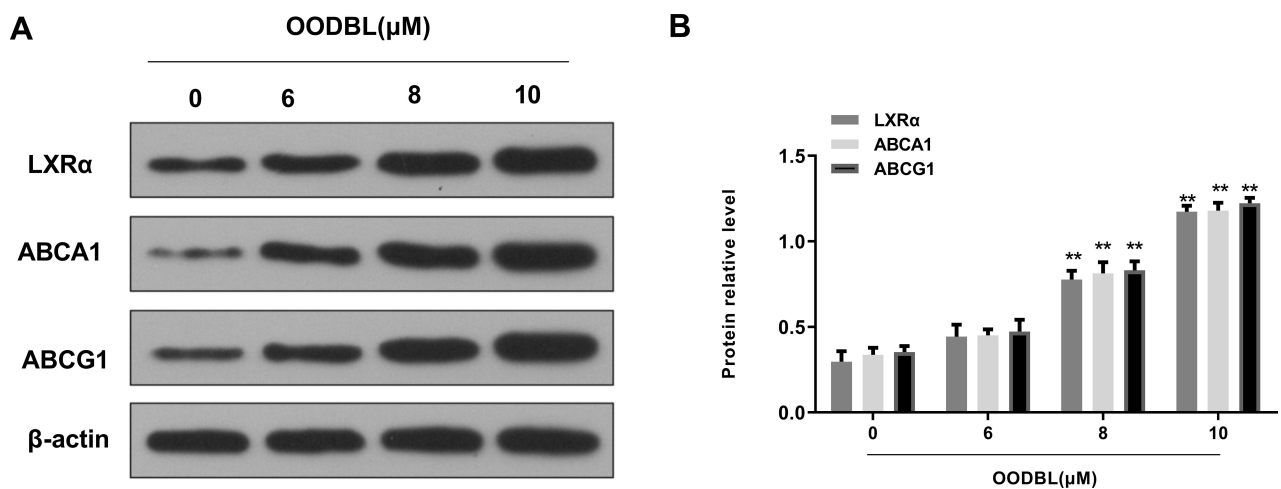


Figure 5 OODBL activates LXRα/ABCA1 signaling. **(A)** The expression levels of LXRα, ABCA1, and ABCG1 were evaluated by Western blot analysis in the CAL27 cells treated with OODBL of indicated dose, in which β-actin was used as an equal loading control. **(B)** The results of Western blot analysis were quantified by ImageJ software. **Notes:** n=3, means ± SD, compared with the control group, ***p* < 0.01.

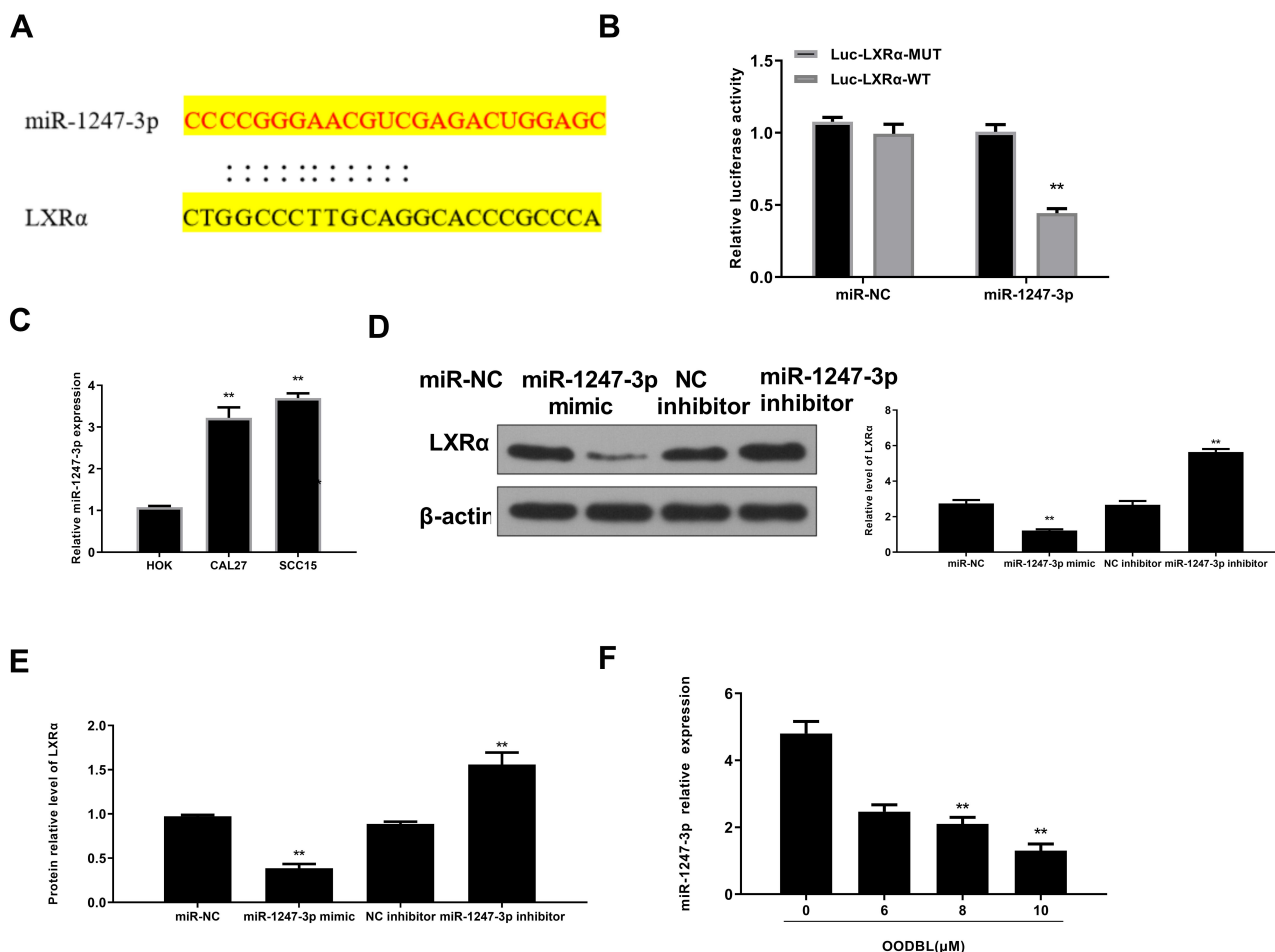


Figure 6 OODBL activates LXR α /ABCA1 signaling by targeting miR-1247-3p. **(A)** The putative targeting sites for LXR α and miR-1247-3p were shown. **(B)** The luciferase activity of wild type LXR α (LXR α -WT) and LXR α with miR-1247-3p binding site mutant (LXR α -Mut) were analyzed by luciferase reporter gene assays in cells treated with control miRNA (miR-NC) or miR-1247-3p mimic. **(C)** The intuitive expression of miR-1247-3p was analyzed by qPCR assays in the cells. **(D)** The protein expression levels of LXR α were measured by Western blot analysis in the CAL27 cells treated with miR-1247-3p mimic or miR-1247-3p inhibitor. The results were quantified by ImageJ software. **(E)** The mRNA expression levels of LXR α were assessed by RT-qPCR in the CAL27 cells treated with miR-1247-3p mimic or miR-1247-3p inhibitor. **(F)** The expression levels of miR-1247-3p was tested by qPCR in the CAL27 cells treated with OODBL of indicated dose.

Notes: n=3, means \pm SD, compared with the control group, ** $p < 0.01$.

OODBL Represses Tumor Growth of OSCC Cells in vivo

To better understand the role of OODBL in the inhibition of OSCC progression in vivo, we performed the tumorigenicity analysis by injecting the CAL27 cells into 4-week-old nude mice. OODBL treatment significantly inhibited tumor growth of CAL27 cells in a dose-dependent manner in vivo, as demonstrated by the significantly decreased tumor size (Figure 8A), tumor weight ($P < 0.01$) (Figure 8B) and tumor volume ($P < 0.01$) (Figure 8C). In addition, immunohistochemical staining further revealed that the expression level of Ki-67 was reduced in the OODBL group (Figure 8D). Moreover, we validated that the protein levels of LXR α , ABCA1, and ABCG1 ($P < 0.01$) were remarkably up-regulated by

OODBL (Figure 8E). Together these data indicate that OODBL represses tumor growth of OSCC cells in vivo.

Discussion

Oral squamous cell carcinoma (OSCC) stands amid the most prevalent cancer globally and is correlated with hard morbidity and enormous mortality.⁴¹ OSCC is a dangerous latent disease because of the approximation of the smooth tissues to the underlying bone, leading to severe skeletal damage and consequent mortality or morbidity in many cases.^{42,43} The oral cavity is continuously endangered to carcinogens such as betel nut, alcohol, and tobacco, causing it is the most usual position for the spring of epithelial malignancy in the neck and head.^{44–46} Although therapeutic improvements, the clinical outcome of this cancer continues stagnant, and the five-year survival frequency is

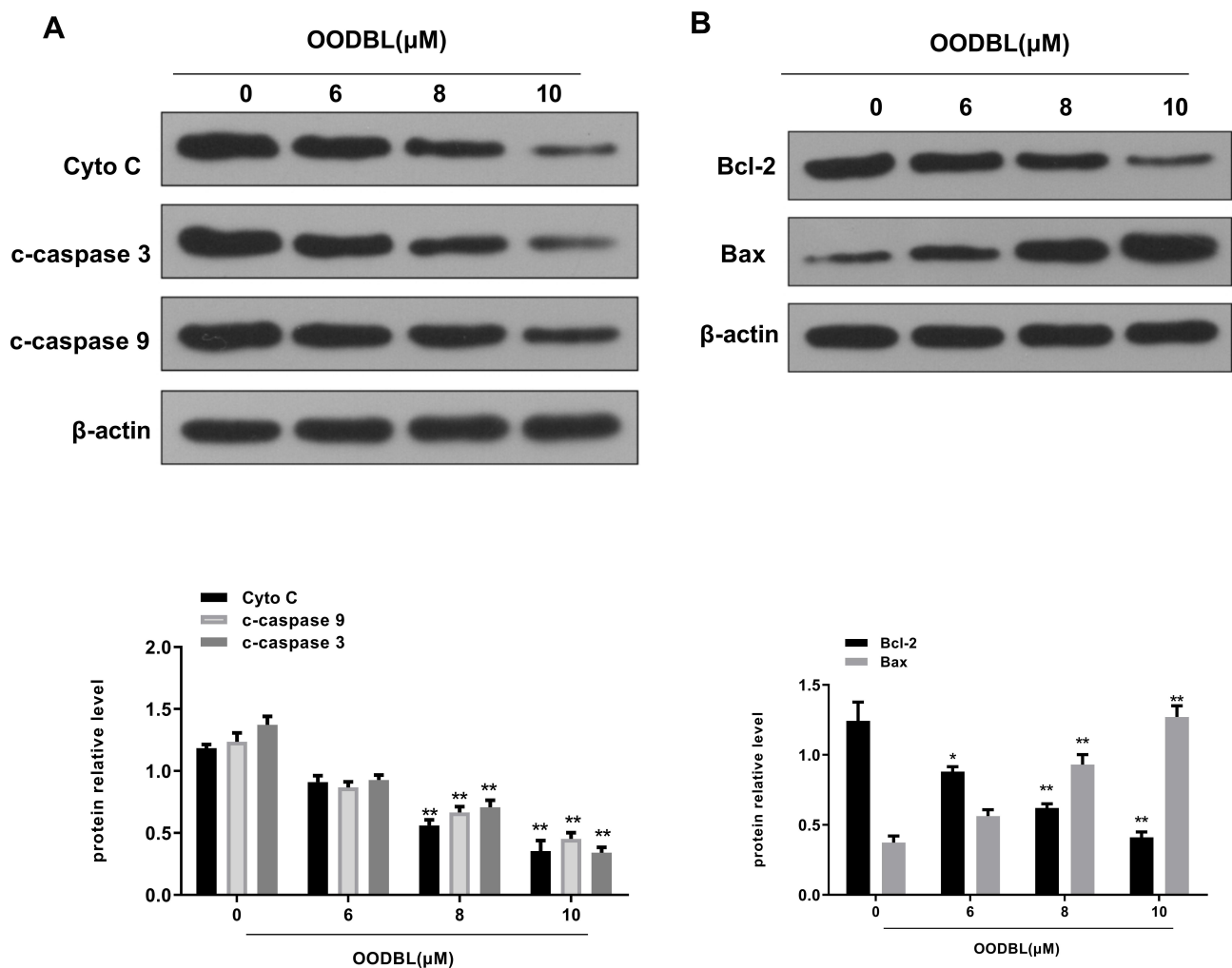


Figure 7 OODBL affects cytochrome C and caspases activities in OSCC cells. **(A)** The expression levels of cytochrome c in the cytoplasm, cleaved caspase-9 (c-caspase-9), and cleaved caspase-3 (c-caspase-3) were analyzed by Western blot analysis in the CAL27 cells treated with OODBL of indicated dose, in which β -actin was used as an equal loading control. The results were quantified by ImageJ software. **(B)** The expression levels of Bcl-2 and Bax were measured by Western blot analysis in the CAL27 cells treated with OODBL of indicated dose, in which β -actin was used as an equal loading control. The results were quantified by ImageJ software.

Notes: n=3, means \pm SD, compared with the control group, * p < 0.05, ** p < 0.01.

approximately 60% throughout the latest decades.^{47–49} Besides, a medical herb of *Inula britannica* has a wide variety of activities such as anti-cancer, antioxidant, anti-inflammatory, and neuroprotective function.⁵⁰ Multiple active compounds from *Inula britannica* have exhibited a practical anti-tumor effect.^{16,51,52} Moreover, it has been reported that OODBL from *Inula britannica* represses the expression of ALOX15 and eotaxin-1 by the STAT6 inactivation.⁵³ In this study, we identified that OODBL was able to inhibit the progression of OSCC in vitro and in vivo. Our study firstly uncovered the anti-tumor effect of OODBL on OSCC, providing new evidence of the cancer inhibitory function of OODBL.

It has been reported that analog ABL-L detached from *Inula britannica* provokes apoptosis of human larynx

carcinoma cells by regulating the p53 pathway.⁵⁴ Two known sesquiterpene lactones, including O, O-diacetylbritannilactone (OODABL) and O-acetylbritannilactone (OABL), activate anti-tumor outcomes rely on the phosphorylation of Bcl-2.⁵⁵ HED isolated from *Inula britannica* advances apoptosis in diffuse large B-cell lymphoma cells.⁵⁶ Furthermore, OODBL causes apoptosis in human leukemia cells by modulating caspases, cytochrome c, Bcl-2, and MAPK.²² Our data demonstrated that OODBL arrested cells to the G0/G1 phase and promoted cell apoptosis in the CAL27 and SCC15 cells. Bcl-2 family, as a crucial antiapoptotic member in carcinogenesis, is correlated to the anti-tumor treatment resistance such as cisplatin.⁵⁷ Stimulation of Bax leads to mitochondrial outer membrane permeabilization (MOMP) and the deliverance of

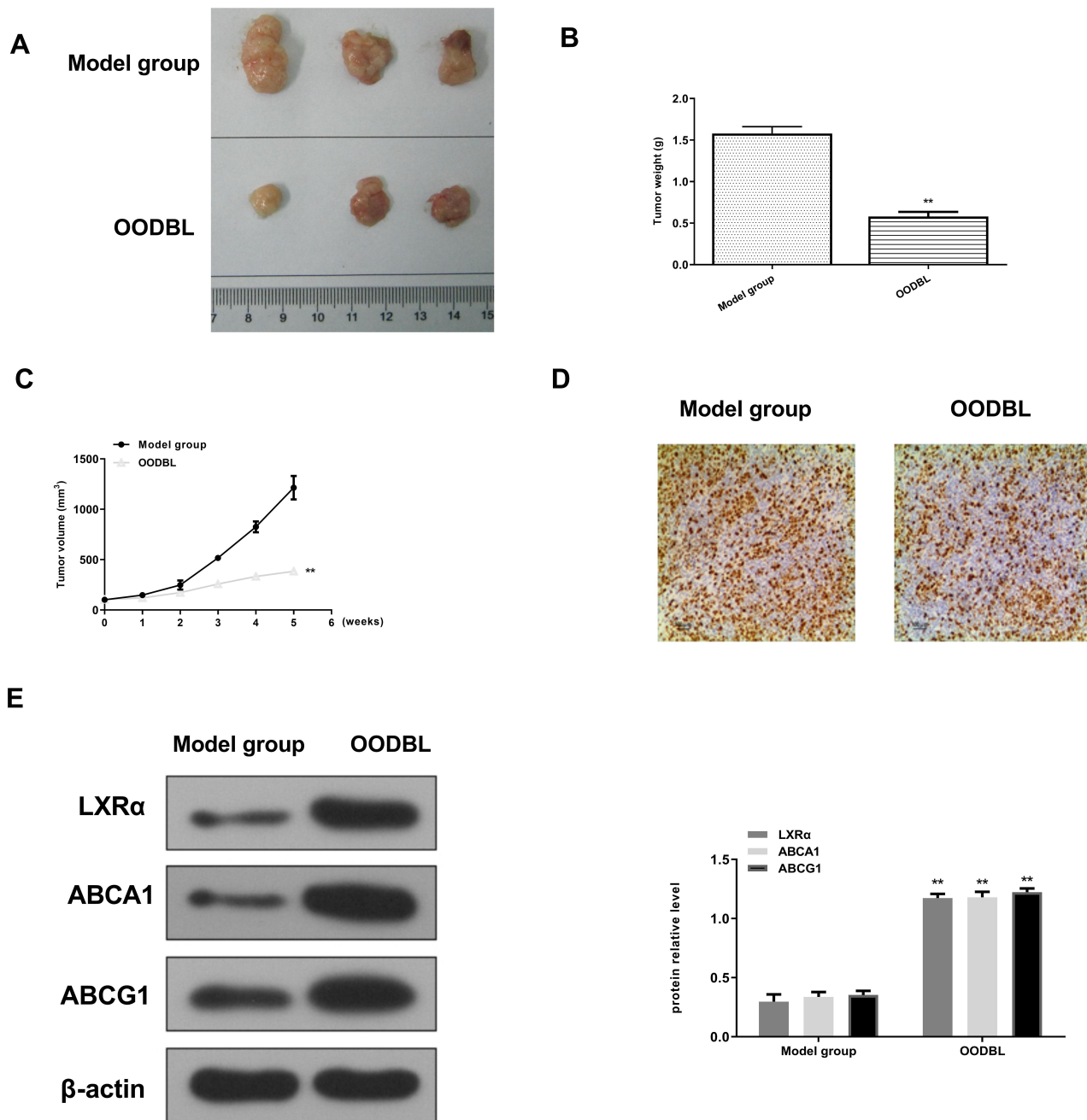


Figure 8 OODBL represses tumor growth of OSCC cells in vivo. **(A–E)** The effect of OODBL in tumor growth of OSCC cells in vivo was analyzed by nude mice tumorigenicity assay. **(A)** Images of dissected tumors from nude mice of the model group and OODBL treatment group (0.1mL/10g). **(B)** The average tumor weight was calculated are shown. **(C)** The average tumor volume was calculated are shown. **(D)** The expression levels of Ki-67 of the tumor tissues were measured by immunohistochemical staining. **(E)** The protein expression levels of LXR α , ABCA1, and ABCG1 were examined by Western blot analysis in the tumor tissues, in which β -actin was used as an equal loading control. The results were quantified by ImageJ software.

Notes: n=3, means \pm SD, compared with the control group. ** $p < 0.01$.

cytochrome c from the inter-membrane space to the cytosol. Cytochrome c can form the apoptosome and cleave the caspase-9 and caspase-3, contributing to the apoptosis in cancer cells.³⁷ We found that OODBL dose-dependently inhibited the expression levels of cytochrome c in the cytoplasm, cleaved caspase-9 (c-caspase-9), and cleaved caspase-

3 (c-caspase-3) in CAL27 cells. And the protein levels of Bcl-2 were reduced, but the Bax levels were enhanced by OODBL in the cells. These data indicate that cytochrome c, c-caspase-9, c-caspase-3, Bcl-2, and Bax may be involved in OODBL-induced OSCC cell apoptosis, providing new evidence of the OODBL function.

It has been revealed that lycopene represses the progression of androgen-dependent human prostate cancer cells by modulating LXR α /ABCA1 signaling.⁵⁸ Doxorubicin reduced the ABCA1 expression through the downregulation of transcriptional factor LXR α in cancer cells.⁵⁹ Systemic inflammation, TNF- α , and IL-1 β influenced by casein injection restrained the expression of ABCA1 and LXR α in hepatic cells.⁶⁰ ABCA1 and ABCG1 are involved in the modulation of prostate cancer epithelial cells.⁶¹ Our data showed that OODBL significantly activated LXR α , ABCA1, and ABCG1 in the CAL27 cells. Besides, it has been reported that miR-1247-3p aggravates cancer-related activation of fibroblasts to promote liver cancer lung metastasis.³⁴ CircRNA UBXN7 blocks cell invasion and growth through sponging miR-1247-3p to improve the expression of B4GALT3 in bladder cancer.⁶² Multiple miRNAs are also reported to participate in the development of OSCC. MiR-137 is down-regulated in the oral squamous cell carcinoma patients and may be served as a diagnostic marker of oral squamous cell carcinoma.⁶³ MiR-34a-5p is correlated with OSCC cell proliferation and invasion.⁶⁴ MiR-196a-5p is involved in DOCK1/BRIC3 signaling-modulated cell apoptosis of OSCC.⁶⁵ MiR-133a-3p reduces oral squamous cell carcinoma by targeting COL1A1.⁶⁶ MiR-10a promotes OSCC cell proliferation by enhancing GLUT1-related glucose metabolism.⁶⁷ MiR-184 plays a crucial role in lncRNA UCA1-mediated OSCC proliferation and cisplatin resistance.⁶⁸ Remarkably, we identified that miR-1247-3p had an LXR α -targeted sequence and decreased the luciferase activity of wild type LXR α but not LXR α with miR-1247-3p binding site mutant in the CAL27 cells. We further verified that the expression levels of LXR α were notably decreased by miR-1247-3p mimic and were remarkably increased by miR-1247-3p inhibitor in the cells. Moreover, OODBL could reduce the expression of the miR-1247-3p in the system. These data suggest that OODBL is able to activate LXR α /ABCA1 signaling by targeting miR-1247-3p. The more profound significance of miR-1247-3p/LXR/ABCA1 in the OODBL-mediated OSCC progression is needed to explore further.

In conclusion, we discovered that OODBL inhibited the progression of OSCC by modulating miR-1247-3p/LXR α /ABCA1 signaling in vitro and in vivo. Our finding provides a new scenario that OODBL represses OSCC development. Therapeutically, OODBL may be applied as a potential anti-tumor candidate of OSCC in clinical treatment strategy.

Disclosure

The authors declare no competing financial or non-financial interests. Shaohua Zheng and Lihua Li contributed equally to this work.

References

- Gao J, Tian G, Han X, Zhu Q. Twentyfour signature genes predict the prognosis of oral squamous cell carcinoma with high accuracy and repeatability. *Mol Med Rep.* 2018;17(2):2982–2990.
- Wyss AB, Hashibe M, Lee YA, et al. Smokeless tobacco use and the risk of head and neck cancer: pooled analysis of US studies in the INHANCE consortium. *Am J Epidemiol.* 2016;184(10):703–716. doi:10.1093/aje/kww075
- Cannonier SA, Gonzales CB, Ely K, Guelcher SA, Sterling JA. Hedgehog and TGFbeta signaling converge on Gli2 to control bony invasion and bone destruction in oral squamous cell carcinoma. *Oncotarget.* 2016;7(46):76062–76075. doi:10.18632/oncotarget.12584
- Zini A, Czerninski R, Sgan-Cohen HD. Oral cancer over four decades: epidemiology, trends, histology, and survival by anatomical sites. *J Oral Pathol Med.* 2010;39(4):299–305. doi:10.1111/j.1600-0714.2009.00845.x
- De Paz D, Kao HK, Huang Y, Chang KP. Prognostic stratification of patients with advanced oral cavity squamous cell carcinoma. *Curr Oncol Rep.* 2017;19(10):65. doi:10.1007/s11912-017-0624-3
- Foschini MP, Morandi L, Marchetti C, et al. Cancerization of cutaneous flap reconstruction for oral squamous cell carcinoma: report of three cases studied with the mtDNA D-loop sequence analysis. *Histopathology.* 2011;58(3):361–367. doi:10.1111/j.1365-2559.2011.03754.x
- Sonalika WG, Amsavardani Tayaar S, Bhat KG, Patil BR, Muddapur MV. Oral microbial carriage in oral squamous cell carcinoma patients at the time of diagnosis and during radiotherapy – a comparative study. *Oral Oncol.* 2012;48(9):881–886. doi:10.1016/j.oraloncology.2012.03.018
- Brinkmann O, Wong DT. Salivary transcriptome biomarkers in oral squamous cell cancer detection. *Adv Clin Chem.* 2011;55:21–34.
- Murthy V, Agarwal JP, Laskar SG, et al. Analysis of prognostic factors in 1180 patients with oral cavity primary cancer treated with definitive or adjuvant radiotherapy. *J Cancer Res Ther.* 2010;6(3):282–289. doi:10.4103/0973-1482.73360
- Elmali A, Yilmaz MT, Yazici G. Challenging the requirement to treat the contralateral neck in cases with >4 mm tumor thickness in patients receiving postoperative radiation therapy for squamous cell carcinoma of the oral tongue or floor of mouth. *Am J Clin Oncol.* 2019;42(2):228. doi:10.1097/COC.0000000000000503
- Hill SJ, D'Andrea AD. Predictive potential of head and neck squamous cell carcinoma organoids. *Cancer Discov.* 2019;9(7):828–830. doi:10.1158/2159-8290.CD-19-0527
- Bae WY, Kim HY, Choi KS, et al. Investigation of brassica juncea, forsythia suspensa, and inula britannica: phytochemical properties, antiviral effects, and safety. *BMC Complement Altern Med.* 2019;19(1):253. doi:10.1186/s12906-019-2670-x
- Zarei M, Mohammadi S, Komaki A. Antinociceptive activity of Inula britannica L. and patuletin: in vivo and possible mechanisms studies. *J Ethnopharmacol.* 2018;219:351–358. doi:10.1016/j.jep.2018.03.021
- Ivanova V, Trendafilova A, Todorova M, Danova K, Dimitrov D. Phytochemical profile of Inula britannica from Bulgaria. *Nat Prod Commun.* 2017;12(2):153–154.
- Kim KC, Kim DJ, Lee MS, Seo JY, Yoo ID, Lee IS. Inhibition of human neutrophil elastase by sesquiterpene lactone dimers from the flowers of Inula britannica. *J Microbiol Biotechnol.* 2018;28(11):1806–1813. doi:10.4014/jmb.1807.07039

16. Seca AM, Grigore A, Pinto DC, Silva AM. The genus *Inula* and their metabolites: from ethnopharmacological to medicinal uses. *J Ethnopharmacol.* 2014;154(2):286–310. doi:10.1016/j.jep.2014.04.010
17. Chen L, Zhang JP, Liu X, Tang JJ, Xiang P, Ma XM. Semisynthesis, an anti-inflammatory effect of derivatives of 1beta-hydroxy alantolactone from *Inula britannica*. *Molecules.* 2017;22(11):1835. doi:10.3390/molecules22111835
18. Khan AL, Hussain J, Hamayun M, et al. Secondary metabolites from *Inula britannica* L. and their biological activities. *Molecules.* 2010;15(3):1562–1577. doi:10.3390/molecules15031562
19. Xiang P, Guo X, Han YY, Gao JM, Tang JJ. Cytotoxic and pro-apoptotic activities of sesquiterpene lactones from *Inula britannica*. *Nat Prod Commun.* 2016;11(1):7–10.
20. Jin M, Kim S, Qin N, et al. 1,6-O,O-Diacetylbritannilactone suppresses activation of mast cell and airway hyper-responsiveness. *Immunopharmacol Immunotoxicol.* 2017;39(4):173–179. doi:10.1080/08923973.2017.1318911
21. Merten J, Wang Y, Krause T, Kataeva O, Metz P. Total synthesis of the cytotoxic 1,10-seco-eudesmanolides britannilactone and 1,6-O, O-diacetylbritannilactone. *Chemistry.* 2011;17(12):3332–3334. doi:10.1002/chem.201002927
22. Pan MH, Chiou YS, Cheng AC, et al. Involvement of MAPK, Bcl-2 family, cytochrome c, and caspases in induction of apoptosis by 1,6-O,O-diacetylbritannilactone in human leukemia cells. *Mol Nutr Food Res.* 2007;51(2):229–238. doi:10.1002/mnfr.200600148
23. Yang CM, Lu YL, Chen HY, Hu ML. Lycopene and the LXRalpha agonist T0901317 synergistically inhibit the proliferation of androgen-independent prostate cancer cells via the PPARgamma-LXRalpha-ABCA1 pathway. *J Nutr Biochem.* 2012;23(9):1155–1162. doi:10.1016/j.jnutbio.2011.06.009
24. Zeng Y, Peng Y, Tang K, et al. Dihyromyricetin ameliorates foam cell formation via LXRalpha-ABCA1/ABCG1-dependent cholesterol efflux in macrophages. *Biomed Pharmacother.* 2018;101:543–552. doi:10.1016/j.biopha.2018.02.124
25. Hu X, Fu Y, Lu X, et al. Protective effects of platycodin D on lipopolysaccharide-induced acute lung injury by activating LXRalpha-ABCA1 signaling pathway. *Front Immunol.* 2016;7:644.
26. Mangum LC, Hou X, Borazjani A, Lee JH, Ross MK, Crow JA. Silencing carboxylesterase 1 in human THP-1 macrophages perturbs genes regulated by PPARgamma/RXR and RAR/RXR: down-regulation of CYP27A1-LXRalpha signaling. *Biochem J.* 2018;475(3):621–642. doi:10.1042/BCJ20180008
27. Ni J, Zhou LL, Ding L, et al. Efatutazone and T0901317 exert synergistically therapeutic effects in acquired gefitinib-resistant lung adenocarcinoma cells. *Cancer Med.* 2018;7(5):1955–1966. doi:10.1002/cam4.1440
28. Wang H, Yang Y, Sun X, et al. Sonodynamic therapy-induced foam cells apoptosis activates the phagocytic PPARgamma-LXRalpha-ABCA1/ABCG1 pathway and promotes cholesterol efflux in advanced plaque. *Theranostics.* 2018;8(18):4969–4984. doi:10.7150/thno.26193
29. Liu B, He Z, Wang J, et al. Taraxasterol inhibits LPS-induced inflammatory response in BV2 microglia cells by activating LXRalpha. *Front Pharmacol.* 2018;9:278. doi:10.3389/fphar.2018.00278
30. Kaneko T, Kanno C, Ichikawa-Tomikawa N, et al. Liver X receptor reduces proliferation of human oral cancer cells by promoting cholesterol efflux via up-regulation of ABCA1 expression. *Oncotarget.* 2015;6(32):33345–33357. doi:10.18632/oncotarget.5428
31. Rupaimoole R, Slack FJ. MicroRNA therapeutics: towards a new era for the management of cancer and other diseases. *Nat Rev Drug Discov.* 2017;16(3):203–222. doi:10.1038/nrd.2016.246
32. Di Leva G, Garofalo M, Croce CM. MicroRNAs in cancer. *Annu Rev Pathol.* 2014;9(1):287–314. doi:10.1146/annurev-pathol-012513-104715
33. Wu Y, Sun X, Song B, Qiu X, Zhao J. MiR-375/SLC7A11 axis regulates oral squamous cell carcinoma proliferation and invasion. *Cancer Med.* 2017;6(7):1686–1697. doi:10.1002/cam4.1110
34. Fang T, Lv H, Lv G, et al. Tumor-derived exosomal miR-1247-3p induces cancer-associated fibroblast activation to foster lung metastasis of liver cancer. *Nat Commun.* 2018;9(1):191. doi:10.1038/s41467-017-02583-0
35. Santucci R, Sinibaldi F, Cozza P, Polticelli F, Fiorucci L. Cytochrome c: an extreme multifunctional protein with a key role in cell fate. *Int J Biol Macromol.* 2019;136:1237–1246. doi:10.1016/j.ijbiomac.2019.06.180
36. Kalpage HA, Bazylanska V, Recanati MA, et al. Tissue-specific regulation of cytochrome c by post-translational modifications: respiration, the mitochondrial membrane potential, ROS, and apoptosis. *FASEB J.* 2019;33(2):1540–1553. doi:10.1096/fj.201801417R
37. Brentnall M, Rodriguez-Menocal L, De Guevara RL, Cepero E, Boise LH. Caspase-9, caspase-3 and caspase-7 have distinct roles during intrinsic apoptosis. *BMC Cell Biol.* 2013;14(1):32. doi:10.1186/1471-2121-14-32
38. Serrano BP, Hardy JA. Phosphorylation by protein kinase A disassembles the caspase-9 core. *Cell Death Differ.* 2018;25(6):1025–1039.
39. Zhang Y, Yang X, Ge X, Zhang F. Puerarin attenuates neurological deficits via Bcl-2/Bax/cleaved caspase-3 and Sirt3/SOD2 apoptotic pathways in subarachnoid hemorrhage mice. *Biomed Pharmacother.* 2019;109:726–733. doi:10.1016/j.biopha.2018.10.161
40. Yao S, Ye J, Yin M, Yu R. DMAMCL exerts antitumor effects on hepatocellular carcinoma both in vitro and in vivo. *Cancer Lett.* 2020;483:87–97. doi:10.1016/j.canlet.2020.04.003
41. Xie X, Wang Z, Chen F, et al. Roles of FGFR in oral carcinogenesis. *Cell Prolif.* 2016;49(3):261–269. doi:10.1111/cpr.12260
42. Lindeboom JA, Mathura KR, Ince C. Orthogonal polarization spectral (OPS) imaging and topographical characteristics of oral squamous cell carcinoma. *Oral Oncol.* 2006;42(6):581–585. doi:10.1016/j.oraloncology.2005.10.014
43. Kar P, Supakar PC. Expression of Stat5A in tobacco chewing-mediated oral squamous cell carcinoma. *Cancer Lett.* 2006;240(2):306–311. doi:10.1016/j.canlet.2005.09.023
44. Shetty SS, Shetty P. Tumour horoscope in young adults. *Oral Oncol.* 2019;89:164. doi:10.1016/j.oraloncology.2018.12.016
45. Karmouta R, Mikailov A. Friable erythema and erosions on the mouth. *Cutis.* 2018;102(2):E5–E6.
46. Perry BJ, Zammit AP, Perry CF. Bringing light to dental trauma and oral cavity cancer-reply. *JAMA Otolaryngol Head Neck Surg.* 2015;141(11):1029–1030. doi:10.1001/jamaoto.2015.2410
47. Chinn SB, Myers JN. Oral cavity carcinoma: current management, controversies, and future directions. *J Clin Oncol.* 2015;33(29):3269–3276. doi:10.1200/JCO.2015.61.2929
48. Jemal A, Bray F, Center MM, Ferlay J, Ward E, Forman D. Global cancer statistics. *CA Cancer J Clin.* 2011;61(2):69–90. doi:10.3322/caac.20107
49. Messadi DV. Diagnostic aids for detection of oral precancerous conditions. *Int J Oral Sci.* 2013;5(2):59–65. doi:10.1038/ijos.2013.24
50. Shi X, Zhang K, Xue N, et al. Differentiation of genuine *Inula britannica* L. and substitute specimens based on the determination of 15 components using LC-MS/MS and principal components analysis. *Food Chem.* 2013;141(4):4019–4025. doi:10.1016/j.foodchem.2013.06.123
51. Dong S, Tang JJ, Zhang CC, et al. Semisynthesis and in vitro cytotoxic evaluation of new analogues of 1-O-acetylbritannilactone, a sesquiterpene from *Inula britannica*. *Eur J Med Chem.* 2014;80:71–82. doi:10.1016/j.ejmech.2014.04.028
52. Bai N, Lai C-S, He K, et al. Sesquiterpene lactones from *Inula britannica* and their cytotoxic and apoptotic effects on human cancer cell lines. *J Nat Prod.* 2006;69(4):531–535. doi:10.1021/mp050437q

53. Chen X, Ji N, Qin N, et al. 1,6-O-Diacetylbritanilactone inhibits eotaxin-1 and ALOX15 expression through inactivation of STAT6 in A549 cells. *Inflammation*. 2017;40(6):1967–1974. doi:10.1007/s10753-017-0637-y
54. Han YY, Tang JJ, Gao RF, Guo X, Lei M, Gao JM. A new semisynthetic 1-O-acetyl-6-O-lauroylbritanilactone induces apoptosis of human laryngocarcinoma cells through p53-dependent pathway. *Toxicol in Vitro*. 2016;35:112–120. doi:10.1016/j.tiv.2016.05.019
55. Rafi MM, Bai NS, Chi Tang H, et al. A sesquiterpenelactone from *Inula britannica* induces anti-tumor effects dependent on Bcl-2 phosphorylation. *Anticancer Res*. 2005;25(1A):313–318.
56. Jang DK, Lee IS, Shin HS, Yoo HM. 2alpha-hydroxyeudesma-4,11(13)-dien-8beta,12-olide isolated from *Inula britannica* induces apoptosis in diffuse large B-cell lymphoma cells. *Biomolecules*. 2020;10(2):324. doi:10.3390/biom10020324
57. Nie C, Luo Y, Zhao X, et al. Caspase-9 mediates puma activation in UCN-01-induced apoptosis. *Cell Death Dis*. 2014;5(10):e1495. doi:10.1038/cddis.2014.461
58. Yang CM, Lu IH, Chen HY, Hu ML. Lycopene inhibits the proliferation of androgen-dependent human prostate tumor cells through activation of PPARgamma-LXRalpha-ABCA1 pathway. *J Nutr Biochem*. 2012;23(1):8–17. doi:10.1016/j.jnutbio.2010.10.006
59. Sharma M, Tuaine J, McLaren B, et al. Chemotherapy agents alter plasma lipids in breast cancer patients and show differential effects on lipid metabolism genes in liver cells. *PLoS One*. 2016;11(1):e0148049. doi:10.1371/journal.pone.0148049
60. Ma KL, Ruan XZ, Powis SH, Chen Y, Moorhead JF, Varghese Z. Inflammatory stress exacerbates lipid accumulation in hepatic cells and fatty livers of apolipoprotein E knockout mice. *Hepatology*. 2008;48(3):770–781. doi:10.1002/hep.22423
61. Trasino SE, Kim YS, Wang TT. Ligand, receptor, and cell type-dependent regulation of ABCA1 and ABCG1 mRNA in prostate cancer epithelial cells. *Mol Cancer Ther*. 2009;8(7):1934–1945. doi:10.1158/1535-7163.MCT-09-0020
62. Liu H, Chen D, Bi J, et al. Circular RNA circUBXN7 represses cell growth and invasion by sponging miR-1247-3p to enhance B4GALT3 expression in bladder cancer. *Aging (Albany NY)*. 2018;10(10):2606–2623. doi:10.18632/aging.101573
63. Sun C, Li J. Expression of MiRNA-137 in oral squamous cell carcinoma and its clinical significance. *J BUON*. 2018;23(1):167–172.
64. Li YY, Tao YW, Gao S, et al. Cancer-associated fibroblasts contribute to oral cancer cells proliferation and metastasis via exosome-mediated paracrine miR-34a-5p. *EBioMedicine*. 2018;36:209–220. doi:10.1016/j.ebiom.2018.09.006
65. Wang L, Wei Y, Yan Y, et al. CircDOCK1 suppresses cell apoptosis via inhibition of miR196a5p by targeting BIRC3 in OSCC. *Oncol Rep*. 2018;39(3):951–966.
66. He B, Lin X, Tian F, Yu W, Qiao B. MiR-133a-3p inhibits oral squamous cell carcinoma (OSCC) proliferation and invasion by suppressing COL1A1. *J Cell Biochem*. 2018;119(1):338–346. doi:10.1002/jcb.26182
67. Chen YH, Song Y, Yu YL, Cheng W, Tong X. miRNA-10a promotes cancer cell proliferation in oral squamous cell carcinoma by upregulating GLUT1 and promoting glucose metabolism. *Oncol Lett*. 2019;17(6):5441–5446.
68. Fang Z, Zhao J, Xie W, Sun Q, Wang H, Qiao B. LncRNA UCA1 promotes proliferation and cisplatin resistance of oral squamous cell carcinoma by suppressing miR-184 expression. *Cancer Med*. 2017;6(12):2897–2908. doi:10.1002/cam4.1253

OncoTargets and Therapy

Publish your work in this journal

OncoTargets and Therapy is an international, peer-reviewed, open access journal focusing on the pathological basis of all cancers, potential targets for therapy and treatment protocols employed to improve the management of cancer patients. The journal also focuses on the impact of management programs and new therapeutic

agents and protocols on patient perspectives such as quality of life, adherence and satisfaction. The manuscript management system is completely online and includes a very quick and fair peer-review system, which is all easy to use. Visit <http://www.dovepress.com/testimonials.php> to read real quotes from published authors.

Submit your manuscript here: <https://www.dovepress.com/oncotargets-and-therapy-journal>

Dovepress